PARTICLE PRODUCTION IN THE CENTRAL REGION AT LHC ENERGIES

C. Merino, C. Pajares, and Yu.M. Shabelski

Departamento de Física de Partículas and
Instituto Galego de Física de Altas Enerxías
Universidade de Santiago de Compostela
Galiza, Spain

Low-x Meeting 2011
3rd-7th June 2011
Santiago de Compostela, Galice, Spain,

-Cross sections

-Inclusive densities in the QGSM

-Baryon/antibaryon asymmetry in the QGSM

-Conclusion

Cross section

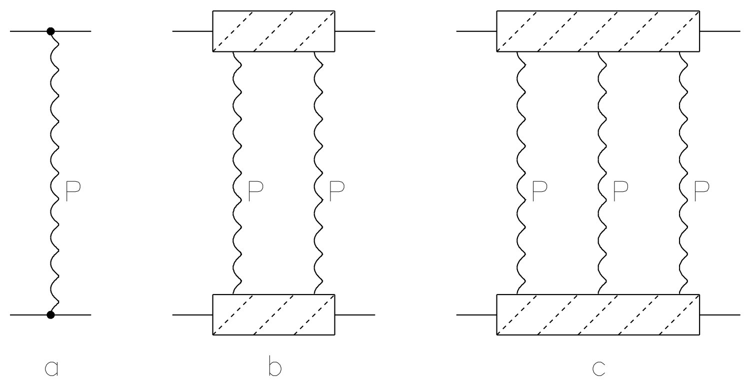

Figure 1: Regge-pole theory diagrams: (a) single, (b) double, and (c) triple Pomeron exchange in elastic hN scattering.

At LHC energies main contribution comes from the exchange of one or several Pomerons. For the Pomeron trajectory

$$\alpha_P(t) = 1 + \Delta + \alpha'_P \cdot t \ , \ \Delta > 0 \ , \qquad (1)$$

the one-Pomeron contribution to σ_{hN}^{tot} equals

$$\sigma_P = 8\pi \cdot \gamma \cdot e^{\Delta \cdot \xi}, \ \text{with} \ \xi = \ln s/s_0 \ , \qquad (2)$$

where γ is the Pomeron coupling, $s_0 \simeq 1$ GeV^2, and σ_P rises with energy as s^{Δ}.

The correct asymptotic behavior $\sigma_{hN}^{tot} \sim \ln^2 s$, can be obtained by taking into account the multipomeron exchanges.

A simple quasi-eikonal treatment yields to

$$\sigma_{hN}^{tot} = \sigma_P \cdot f(z/2) \ , \quad \sigma_{hN}^{el} = \frac{\sigma_P}{C} \cdot [f(z/2) - f(z)] \ , \quad (3)$$

$$f(z) = \frac{1}{z} \int_0^z \frac{dx}{x} \cdot (1 - e^{-x}) \ , \quad (4)$$

$$z = \frac{2C \cdot \gamma}{\lambda} \cdot e^{\Delta \xi} \ , \ \lambda = R^2 + \alpha'_P \cdot \xi \ . \quad (5)$$

Here, R^2 is the radius of the Pomeron and C is the quasi-eikonal enhancement coefficient.

The numerical values of the Pomeron parameters were taken to be :

$$\begin{aligned} \Delta &= 0.139, \ \ \alpha'_P = 0.21 \, \mathrm{GeV}^{-2}, \quad (6) \\ \gamma &= 1.77 \, \mathrm{GeV}^{-2}, \ \ R^2 = 3.18 \, \mathrm{GeV}^{-2}, \ \ C = 1.5. \end{aligned}$$

The predictions of Regge theory are presented in Table 1 together with the experimental data by ATLAS

ATLAS Collaboration, arXiv:1104.0326 [hep-ex]

$\sqrt{s}$	σ^{tot}	σ^{el}	σ^{inel}	σ^{inel}(ATLAS)
900 GeV	67.4	13.2	54.2	
7 TeV	94.5	21.1	73.4	69.4 ± 2.4
14 TeV	105.7	24.2	81.5	

Table 1. The Regge theory predictions for the integral cross sections (in mb) in pp collisions at LHC energies.

In the complete Regge theory more complicated (enhanced) diagrams should be taken into account.

The numerical calculations which account for them lead to values of σ_{pp}^{inel} of the same order ($\pm$ 10% at $\sqrt{s} = 14$ TeV) as those presented in Table 1.

V.A. Khoze, A.D. Martin, and M. G. Ryskin, Eur. Phys. J. **C54**, 199 (2008); **C60**, 249 (2009)

E. Gotsman, E. M. Levin, U. Maor, and J.S. Miller, Eur. Phys. J. **C57**, 689 (2008)

S. Ostapchenko, arXiv: 1003.0196 [hep-ph]

Inclusive densities in the QGSM

The Quark-Gluon String Model (QGSM) is based on Regge phenomenology and it is successfully used for the description of multiparticle production processes.

A.B. Kaidalov and K.A. Ter-Martirosyan, Yad. Fiz. **39**, 1545 (1984); **40**, 211 (1984)

In the QGSM high energy interactions are considered as proceeding via the exchange of one or several Pomerons, and all elastic and inelastic processes result from cutting through or between Pomerons.

V.A. Abramovsky, V.N. Gribov, and O.V. Kancheli, Yad. Fiz. **18**, 595 (1973)

The Inclusive spectra of hadrons are related to the corresponding fragmentation functions of quarks and diquarks, which are constructed using the Reggeon counting rules.

A. B. Kaidalov, Sov. J. Nucl. Phys. **45**, 902 (1987)

Each Pomeron corresponds to a cylindrical diagram Fig. 2a, and thus, when cutting one Pomeron, two showers of secondaries are produced as it is shown in Fig. 2b.

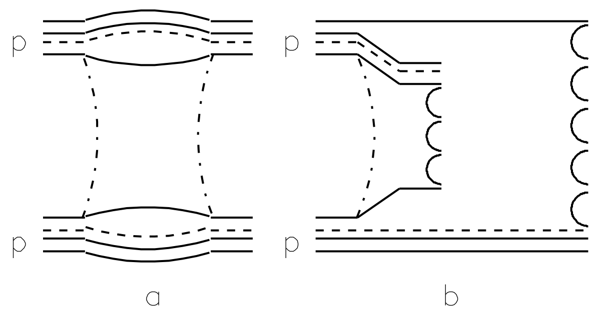

Figure 2: (a) Cylindrical diagram corresponding to the one–Pomeron exchange, and (b) the cut of this diagram which determines the contribution to the inelastic pp cross section.

The inclusive spectrum of a secondary hadron h is then determined by the convolution of the diquark and quark distributions $u(x, n)$ in the incident particles, with the fragmentation functions $G^h(z)$ of diquarks and quarks into the secondary hadron h.

The cut of several Pomerons leads to the production of several pairs of showers.

The comparison of our predictions

C. Merino, C. Pajares, M.M. Ryzhinskiy and Yu.M. Shabelski, arXiv:1007.3206 [hep-ph]

and the most recent data by the ALICE Collaboration

K. Aamodt et al., ALICE Collaboration, arXiv: 1101.4110 [hep-ex]

is presented in Table 2.

Particle	QGSM	ALICE Collaboration
π^+	1.68	$1.493 \pm 0.004 \pm 0.074$
π^-	1.66	$1.485 \pm 0.004 \pm 0.074$
K^+	0.17	$0.184 \pm 0.004 \pm 0.015$
K^-	0.16	$0.183 \pm 0.004 \pm 0.015$
$\overline{p}$	0.10	$0.077 \pm 0.002 \pm 0.006$
$\overline{\Lambda}$	0.05	0.08
$\overline{\Xi^+}$	0.005	0.009
$\overline{\Omega^+}$	0.0004	0.0008

Table 2. The QGSM predictions for the midrapidity yields dn/dy ($|y| < 0.5$) of different secondaries at energy $\sqrt{s} = 900$ GeV together with the experimental data by the ALICE Collaboration.

Our prediction for the value of the ratio of Ξ^-/Λ midrapidity yields ~ 0.10

C. Merino, C. Pajares, M.M. Ryzhinskiy and Yu.M. Shabelski, arXiv:1007.3206 [hep-ph]

is in agreement with the experimental result by the ALICE Collaboration $\Xi^-/\Lambda \simeq 0.11 \pm 0.05$

H. Oeschler et al., ALICE Collaboration, arXiv: 1102.2745 [hep-ex].

We predict for all inelastic interactions one increase of the midrapidity yields for π and K mesons by a factor 1.4 times in the energy region $\sqrt{s} = 900$ GeV−7 TeV, smaller than the experimental increase $1.69 \pm 0.01 \pm 0.06$ in the data for K_s^0 for NSD events.

CMS Collaboration, arXiv: 1102.4282 [hep-ex]

For antibaryons we predict increases in the range from ~ 1.6 for $\bar{p}$ and $\bar{\Lambda}$ to ~ 2.0 for $\overline{\Omega}$.

Baryon/antibaryon asymmetry in QGSM

In the string models baryons are considered as configurations consisting of three connected strings (related to three valence quarks) called string junction (SJ) (see Fig. 3).

G.C. Rossi and G. Veneziano, Nucl. Phys. B **123**, 507 (1977)

Such a baryon structure is supported by lattice calculations.

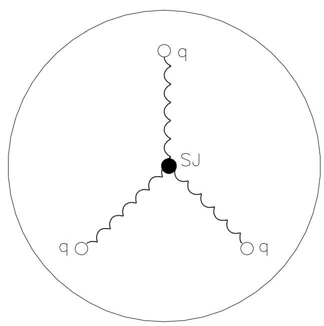

Figure 3: The composite structure of a baryon in string models. Quarks are shown by open points and SJ by black point.

The production of a baryon-antibaryon pair in the central region usually occurs via SJ-$\overline{SJ}$ pair production (see Fig. 4a).

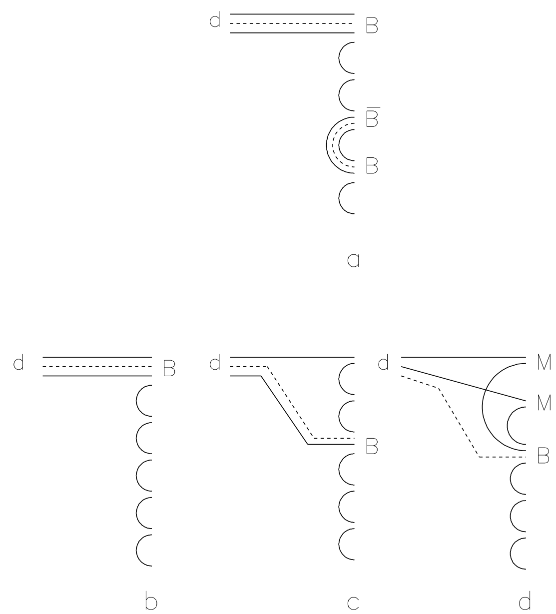

Figure 4: (a) Central production of $\overline{B}B$ pair. Single production of B in the processes of diquark fragmentation: initial SJ together with (b) two valence quarks and one sea quark, together with (c) one valence quark and two sea quarks, and together with (d) three sea quarks.

For pp collisions, another possibility to produce a secondary baryon in the central region is shown in Fig. 4d.

B.Z. Kopeliovich and B. Povh, Z. Phys. C **75**, 693 (1997); Phys. Lett. B **446**, 321 (1999)

G.H. Arakelyan, A. Capella, A.B. Kaidalov, and Yu.M. Shabelski, Eur. Phys. J. C **26**, 81 (2002)

The three processes shown in Figs. 4b-d are determined by the following fragmentation functions:

$$G_{qq}^{B}(z) = a_N \cdot v_{qq}^{B} \cdot z^{2.5} \,, \quad (7)$$

$$G_{qs}^{B}(z) = a_N \cdot v_{qs}^{B} \cdot z^{2} \cdot (1-z) \,, \quad (8)$$

$$G_{ss}^{B}(z) = a_N \cdot \varepsilon \cdot v_{ss}^{B} \cdot z^{1-\alpha_{SJ}} \cdot (1-z)^2 \,. \quad (9)$$

The processes Fig. 4b and 4c contribute to the baryon production in the fragmentation region.

The contribution shown in Figure 4d is essential if the intercept of the SJ exchange Regge-trajectory, α_{SJ}, is large enough and it is weighted by a coefficient ε determines the small probability for such a baryon number transfer to occur.

This contribution takes the baryon number to the central region.

The data by the ALICE Collaboration for $\bar{p}/p$ ratios in pp collisions at $\sqrt{s} = 900$ GeV and 7 TeV are presented in Table 3, together with the QGSM results.

K. Aamodt et al., ALICE Collaboration, Phys. Rev. Lett.**105**, 072002 (2010)

for $\bar{p}/p$ ratios in pp collisions at $\sqrt{s} = 900$ GeV and 7 TeV are presented in Table 4. together with QGSM results.

SJ exchange	$\sqrt{s} = 900$ GeV	$\sqrt{s} = 7$ TeV
$\alpha_{SJ} = 0.9$	0.89	0.95
$\alpha_{SJ} = 0.5$	0.95	0.99
$\varepsilon = 0$	0.98	1.
ALICE Collaboration	$0.957 \pm 0.006 \pm 0.014$	$0.991 \pm 0.005 \pm 0.014$

Table 3. The QGSM predictions for $\bar{p}/p$ in pp collisions at LHC energies and the data by the ALICE Collaboration. The value $\varepsilon = 0$ corresponds to the case with not C-negative exchange.

The LHCb Collaboration measured the ratios of $\bar{\Lambda}$ to Λ in the rapidity interval $2 < y < 4$ at $\sqrt{s} = 900$ GeV and 7 TeV

F. Dettori et al., LHCb Collaboration, Nucl. Phys. B (Proc. Suppl.) **206-207**, 351 (2010)

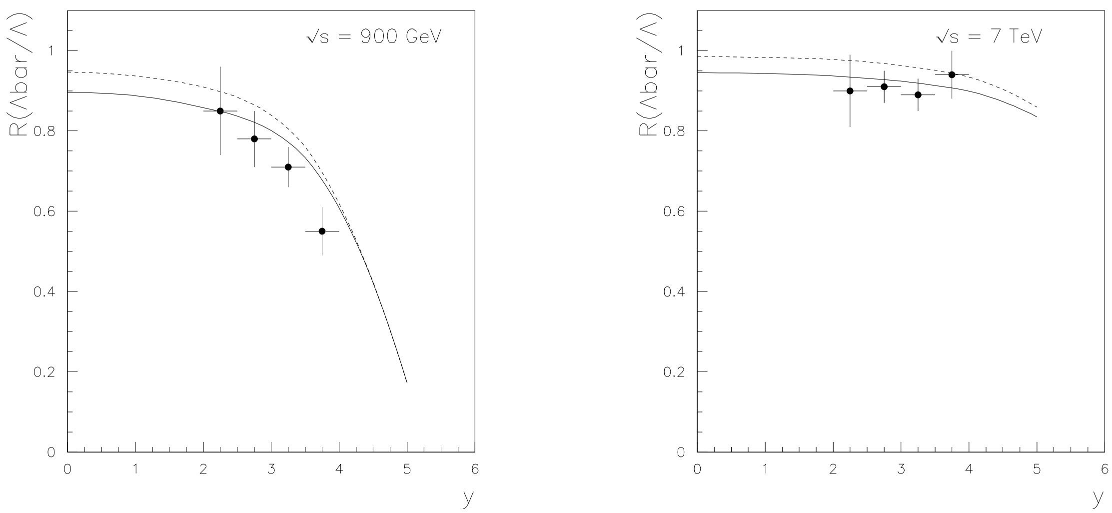

Figure 5: The QGSM predictions (solid curves for $\alpha_{SJ} = 0.9$ and dashed curves for $\alpha_{SJ} = 0.5$) for the $\bar{\Lambda}$ to Λ ratios, as the functions of their rapitities at $\sqrt{s} = 900$ GeV (left) and $\sqrt{s} = 7$ TeV (right), together with the data by the LHCb Collaboration.

Though the errorbars are too large, the QGSM calculations with the value $\alpha_{SJ} = 0.9$ seem to be in a slightly better agreement with the data.

Conclusion

The first experimental data obtained at LHC fot the inelastic cross section, inclusive densities of secondaries, and $\bar{B}/B$ ratios are in reasonable agreement with the calculations provided by QGSM

The values of parameters in the model are those already fixed at lower energies, mainly for the description of the data of fixed target experiments.